Proceedings of the 35th European Safety and Reliability & the 33rd Society for Risk Analysis Europe Conference
Edited by Eirik Bjorheim Abrahamsen, Terje Aven, Frederic Bouder, Roger Flage, Marja Ylönen

doi: 10.3850/978-981-94-3281-3_ESREL-SRA-E2025-P4726-cd

Derivation of an Updated Aging Curve for Polycarbonate Vision Panels Used as Safeguards in Machine Tools

Eckart Uhlmann[1,2], Mitchel Polte[1,2], Nils Bergström[1]

[1] *Institute for Machine Tools and Factory Management IWF, Technische Universität Berlin, Germany, E-mail: bergstroem@iwf.tu-berlin.de*

[2] *Fraunhofer Institute for Production Systems and Design Technology IPK, Berlin, Germany.*

Dietmar Auhl[3], Justus Schönebeck [3], Magdalena Goslinska[3], Oliver Löschke[3], Eduardo Filipetto[3]

[3] *Department of Polymer Materials and Technology, Technische Universität Berlin, Germany.*

Safety regulations for machine tools require an adequate protection of operators from potential hazards, such as ejected workpiece or tool fragments. To meet these requirements, machine tool manufacturers implement different safety measures. A key component of these measures are polycarbonate (PC) vision panels, which provide essential protection while allowing the operator to observe the machining process. Newly manufactured PC is characterized by its high ductility allowing it to absorb impacts with substantial kinetic energy from ejected parts in the event of an accident. However, exposure to cooling lubricant (CL)-water mixtures cause the onset of degradation processes, which result in the accelerated aging of the material. The degradation progressively reduces the protective performance of PC vision panels, limiting their long-term effectiveness as a safeguard. This behavior is accounted for in the design of PC vision panels by using an aging curve defined in international standards. Nevertheless, the aging curve has become outdated due to the implementation of the REACH regulation, which has caused a significant change in the composition of CL. This paper proposes a new aging curve for REACH-compliant, mineral oil-based, amine-containing, and boron-free CL. The updated aging curve is derived from accelerated aging experiments conducted under elevated temperatures and CL concentrations. It is demonstrated how the results of accelerated aging procedures can be translated to industrial operating conditions in machine tools. The PC specimens were analyzed by means of Charpy and safeguard impact tests according to ISO 23125. For the first time, the proposed aging curve facilitates the assessment of PC vision panel aging under REACH-compliant CL. Furthermore, the established procedure provides a framework for deriving additional aging curves for other CL formulations.

Keywords: Safety, Machine tools, Polycarbonate, Aging, Cooling lubricants, S-N curve.

1. Introduction

Efforts to predict the service lifetimes of machinery and device components have been ongoing for nearly two centuries (Schütz 1996). The origins can be traced back to ALBERT'S work in 1837 (1837), in which the fatigue failure of conveyor chains was studied. This foundational work was followed by WÖHLER'S pioneering research on the fatigue of railway axles (1858; 1860), which not only laid the groundwork for the modern understanding of material fatigue but also introduced the concept of S-N curves to characterize the relationship between applied stress (S) and the number of cycles to failure (N). As material science advanced and polymers were introduced into engineering, the fatigue behavior of this novel class of material became a focus of scientists and engineers and has been studied ever since (Starkova et al. 2022). Regardless of the type of material, the fundamental approach for predicting fatigue and estimating remaining service life is largely based on the use of S-N curves (Burhan and Kim 2018). However, in some cases, service life predictions are not governed by cyclic mechanical loading but by cyclic exposure to deteriorating environmental conditions. The aging curve of polycarbonate (PC) vision panels used as safeguards in machine tools is one such example. When PC vision panels are exposed to cooling lubricant (CL)-water mixtures, their ability to retain ejected workpiece or tool fragments in the event of an accident is reduced significantly (Uhlmann et al. 2023; Bold 2004). The aging curve reflects this reduction in protective performance due to prolonged CL exposure and it has been incorporated into international safety standards for machine tools, such as ISO 14120 (ISO 14120) and ISO 23125 (ISO 23125). Despite its crucial role in machine tool safety, the scientific basis of the aging curve remains surprisingly under-documented. The only reference known to the authors was found in Ising (1997), which further refers to "unpublished studies" of Sege Sicherheitsfenster GmbH, Stuttgart, Germany, Index-Werke GmbH & Co. KG, Esslingen, Germany and the German Social Accident Insurance (DGUV), Sankt Augustin, Germany. This fact, along with the introduction of the REACH-regulation in 2016, which lead to the reformulation of most CL, underscores the necessity for a transparent development of a new aging curve for PC vision panels in machine tools. Hence, this paper proposes the derivation of an updated aging curve using two aging procedures: an accelerated procedure and one conducted under industrial operating conditions. For the latter, machine tools from the participating companies Ahlberg Engineering GmbH (Ahlberg), Berlin, Germany and Röders GmbH (Röders), Soltau, Germany were used. Aging effects were assessed using Charpy impact tests and safeguard impact tests according to ISO 23125. The findings of this study contribute to the development of an updated aging curve for PC vision panels in machine tools. Moreover, the proposed procedures establish a framework for deriving further aging curves for other CL formulations.

2. Experimental procedures and data analysis

2.1 Aging procedures

This study employed two approaches to aging: an accelerated aging procedure, where environmental parameters were elevated beyond those typically found in standard machine tools, and a second approach in which PC was subjected to the industrial operating conditions of machine tools. The accelerated procedure aims to predict the long-term effects of CL exposure, while the second approach serves to correlate accelerated aging results with the natural conditions found in machine tools.

<u>Accelerated aging</u>

Accelerated aging was conducted using a self-built aging tank, shown in Fig 1.

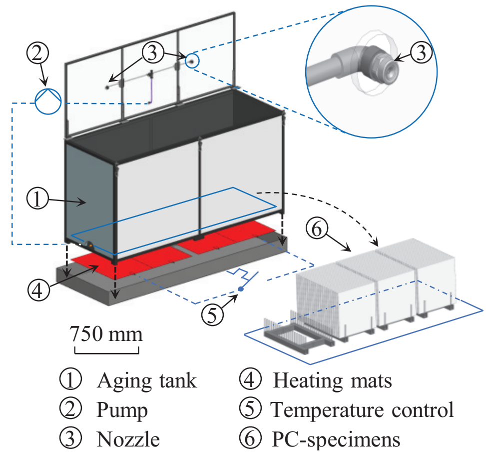

Fig 1. Experimental setup of accelerated aging.

PC specimens were placed inside an aging tank, which was equipped with a pump to circulate a CL-water mixture from the bottom to two nozzles positioned at the of the tank. The pump was time-controlled, enabling intermittent sprinkling of the PC specimen at intervals of $t_i = 10$ min/h. A model CL, defined by the Verband Schmierstoff Industrie e. V. (VSI) was used in this study. The selected CL, designated as VSI 034, represents a typical composition of a water-miscible, mineral oil-based, amine-containing boron-free CL with an elevated pH. The mixture consisted of 30 % VSI 034 and 70 % water and was maintained at a constant temperature of $\vartheta = 45$ °C using heating mats and a temperature control unit. Two types of PC specimen were exposed over total exposure time of $t_{exp} = 78$ weeks to the CL-mixture: Charpy specimens and quadratic PC sheets with a width of $w_{pc} = 500$ mm and a thickness of $t_{pc} = 12$ mm.

<u>Aging under industrial operating conditions</u>

For this aging procedure, Charpy specimens were placed at representative positions within machine tools from the companies Ahlberg and Röders. Figure 2 illustrates the attachment of the specimens inside the machine tool. Since the machine tools were actively used for production tasks, there was insufficient space to accommodate larger PC sheets. Both companies utilized a commercial CL comparable to VSI 034, characterized by being water-miscible, mineral oil-based, amine-containing, boron-free, and

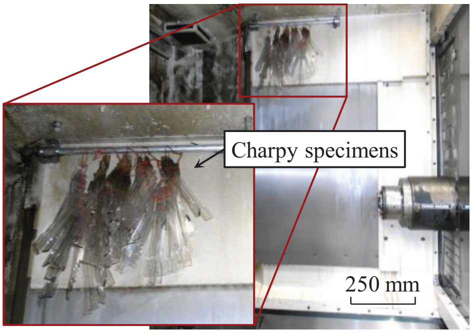

Fig 2. Attachment of Charpy specimens in machine tool.

having an elevated pH. With a composition of 10 % CL and 90 % water, the CL concentration σ differed from the mixtures used in the accelerated aging procedure. Similarly, the temperature within the machine tools, as reported by the participating companies, was approximately $\vartheta = 25$ °C. Both companies kept the specimen for a total exposure time of $t_{exp} = 60$ weeks in their respective machine tools.

2.2 Impact tests

Two types of impact tests were carried out to determine the response of the PC specimen to the CL exposure: Charpy impact tests and safeguard impact tests in accordance with ISO 23125.

Charpy impact tests

An HIT 5.5PF impact tester from ZWICKROELL GMBH & CO. KG, Ulm, Germany was used for the experiments. Notched Charpy specimens of type A in accordance with ISO 179-1 (ISO 179-1) were tested to determine the Charpy impact strength (CIS) a_{cN}.

Safeguard impact tests

The INSTITUTE OF MACHINE TOOLS AND FACTORY MANAGEMENT (IWF) houses a test facility for impact testing on safeguards. For these experiments, a projectile with a mass of $m_{pr} = 2.5$ kg as specified in ISO 23125 (ISO 23125) was accelerated towards the PC sheets in a barrel connected to a pressurized gas tank. A detailed description of the gas canon is provided by UHLMANN ET AL. (2024). The protective performance of the PC sheets was evaluated using regression approach based on RECHT AND IPSON (1963) and LAMBERT AND JONAS (1976). To apply this approach, the initial projectile velocity $v_{pr,i}$ prior to penetrating the PC sheets and the post-penetration velocity $v_{pr,p}$ after penetrating the PC sheets were measured. The projectile velocities are related as shown in Eq. (1), where the a, p and the ballistic limit velocity (BLV) v_{bl} are coefficients that are determined using a least square fit.

$$v_{pr,p} = a \cdot \left(v_{pr,i}^{p} - v_{bl}^{p}\right)^{1/p} \tag{1}$$

Finally, the protective performance of the PC sheets is evaluated based on the BLV v_{bl}. It is defined as initial projectile velocity $v_{pr,i}$ required to emerge from the sheet with a post-penetration projectile velocity of $v_{pr,p} = 0$ m/s (Ben-Dor et al. 2006). To determine the BLV v_{bl} a test series with $n = 10$ impact tests was carried out. Figure 3 provides an illustrative example of such an impact test series and the approximated BLV v_{bl}.

2.3 S-N curves

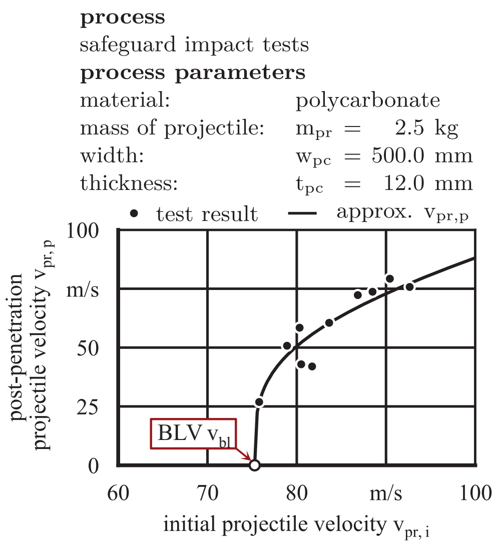

Fig 3. Results of an impact test series.

Given the long history of S-N curves, numerous models have been developed to predict the service life of machinery components. In a comparative study, BURHAN AND KIM (2018) evaluated the effectiveness of nine different models in estimating the remaining operational lifespan of these components. Among these, the models proposed by WEIBULL (1952), SENDECKYJ (1981) and KIM AND ZHANG (2001) demonstrated the highest fitting accuracy for experimental fatigue data. The WEIBULL model, being the most straightforward and practical among the evaluated options, was adopted in this study. Its simplicity, combined with its demonstrated ability to effectively describe the experimental data, makes it a suitable choice for this analysis. The adopted model is presented in Eq. (2), where the parameter x serves as a placeholder for either the CIS a_{cN} or the BLV v_{bl}. Here x_0 denotes the initial value of unaged PC, while t_u is the time of usage, and α, β are the model fitting parameters. The term x_∞ denotes the fatigue lower limit and represents the lower boundary to which the model converges for $t_u \rightarrow \infty$.

$$x(t_u) = (x_0 - x_\infty) \cdot \exp\left(-\alpha \cdot t_u^\beta\right) + x_\infty \qquad (2)$$

Of the aforementioned parameters, only α and β are estimated using a least square fit. Reasonable assumptions and transformations are required for the remaining parameters. Starting with the time of usage t_u: S-N curves are typically based on a specific time scale. Although the exposure time t_{exp} is a viable choice, it fails to capture important nuances, such as the fact that the machine tools were not operated continuously, and the PC specimens were only sprinkled periodically at set intervals t_i. Therefore, the time of usage t_u is defined as actual period in which the PC specimens were in contact with the CL. For aging under industrial conditions, the time of usage t_u corresponds to the operating time of the machine tool, as recorded by the respective company. In the case of the accelerated aging the time of usage t_u is defined as shown in Eq. (3).

$$t_u = t_{exp} \cdot 7 \cdot 24 \cdot t_i \qquad (3)$$

Similar to the current aging curve in ISO standards the aging curve presented in this paper will be defined on a scale from 0 % to 100 %, rather than using the actual values for CIS a_{cN} or the BLV v_{bl}. To achieve this, the quantities were normalized relative to their value at a time of usage $t_u = 0$ h, as exemplified for the normalized CIS $a_{cN,n}$ in Eq. (4).

$$a_{cN,n} = a_{cN} \,/\, a_{cN}\,(t_u = 0\text{h}) \qquad (4)$$

This approach allows for a more generalized application of the aging curve, particularly with respect to the BLV v_{bl}, since the BLV v_{bl} of PC sheets is significantly influenced by their width w_{pc} and thickness t_{pc} (Uhlmann et al. 2021). According to this, the term x_0 of unaged PC is set to $x_0 = 100$ %. The fatigue lower limit x_∞ is determined based in the experimental findings as will be discussed in the following section.

2. Results and discussion

This section demonstrates the derivation of a new aging curve for PC vision panels used as safeguards in machine tools. The derivation is primarily based on the results of Charpy impact tests. It will be shown how the fatigue lower limit x_∞ for both Charpy and safeguard impact tests can be defined using the results from Charpy impact tests. Additionally, these results will be used to derive shift factors that compensate for the elevated temperature ϑ and CL concentration σ in the accelerated aging procedure, enabling the mapping of the experimental data onto industrial operating conditions.

Charpy impact tests

Figure 4 shows the Charpy impact tests results for both the accelerated aging procedure and the aging under industrial operating conditions. In all cases a degradation of the normalized CIS $a_{cN,n}$ is observed, with the most pronounced decrease occurring under accelerated aging conditions where the normalized CIS $a_{cN,n}$ falls to approximately 60 % of its initial value at $t_u = 0$ h. As expected, the degradation under industrial operating conditions is less severe, with values decreasing to 80 % or 86 % of the initial normalized CIS $a_{cN,n}$.

Alongside the test results the fitted aging curve for each group is displayed. To apply the model presented in Eq. (2) a fatigue lower limit $a_{cN,n\infty}$ had to be defined first. From Fig 4 it is evident that the fatigue lower limit $a_{cN,n\infty}$ in terms of mean value has not been reached in any of the experiments. However, single Charpy impact tests with particularly low normalized CIS $a_{cN,n}$ tend to cluster around $a_{cN,n} = 18.5$ % across all aging procedures, suggesting it as a general lower bound. In the absence of any other physically motivated value the fatigue lower limit is thus set to $a_{cN,n} = 18.5$ %. The model parameters for the individual aging curves are presented in Table 1.

Table 1. Coefficients of aging curves.

	acc. Aging	Ahlberg	Röders
$a_{cN,n0}$	1.00	1.00	1.00
$a_{cN,n\infty}$	$1.85 \cdot 10^{-2}$	$1.85 \cdot 10^{-2}$	$1.85 \cdot 10^{-2}$
α	$4.80 \cdot 10^{-9}$	$1.79 \cdot 10^{-5}$	$1.45 \cdot 10^{-5}$
β	2.48	1.22	1.01

<u>Derivation of shift factors</u>

To correlate the results from the accelerated aging procedure with those obtained under industrial operating conditions, characterized by a temperature of $\vartheta = 25$ °C and a CL concentration of $\sigma = 10$ %, shift factors must be defined. Given that one of the primary objectives of this study is to establish a general framework for deriving aging curves applicable to a wide range of CL formulations, including non-water-miscible variants, the effects of elevated temperature ϑ and CL concentration σ are treated separately.

To account for the effects of elevated temperatures ϑ, the ARRHENIUS model is employed, which is widely used for polymeric materials tested under such conditions (Collins et al. 2013). According to the ARRHENIUS model the temperature shift factor f_t is calculated as shown in Eq. (5).

$$f_t = \exp[E_a/R \cdot (1/\vartheta_2 - 1/\vartheta_1)] \qquad (5)$$

In Eq. (5) E_a represents the activation energy, R the universal gas constant, ϑ_1 and ϑ_2 are the elevated and reference temperature, respectively. While the values for the universal gas constant R and the temperatures ϑ_1 and ϑ_2 are known, the activation energy E_a must be determined based on the reactions that drive the aging of PC under exposure to CL. Hydrolysis and aminolysis were identified as primary aging mechanisms under the experimental conditions. While hydrolysis is a common degradation pathway for polymers in alkaline aqueous environments (Ehrenstein and Pongratz 2007), the observed aminolysis reaction is likewise consistent with the findings of FAULKNER (1986), who investigated the aging of PC exposed to amine-containing fluids. In the absence of published data on the activation energy E_a for aminolysis of PC in amine-containing environments, the well-documented hydrolysis parameters provide the best available approximation. Consequently, the activation energy E_a for hydrolysis is adopted for the subsequent analysis. A more detailed examination of these mechanisms will be presented in future work, as it is beyond the scope of this study. The results of a literature review on the activation energy E_a of hydrolysis and the adopted average activation energy $\overline{E}_a$ is presented in Table 2.

Table 2. Activation energy E_a for hydrolysis reaction.

activation energy E_a in kJ/mol
77 (Golovoy and Zinbo 1989)
65 (Kahlen et al. 2010)
92 (Pickett and Coyle 2013)
average activation energy $\overline{E}_a$ = 78 kJ/mol

Using a universal gas constant of $R = 8.314 \cdot 10^{-3}$ kJ/mol·K and the temperatures ϑ described in Section 2.1, the temperature shift factor is calculated as $f_t = 1.38 \cdot 10^{-1}$.

While increasing the temperature ϑ is a common method for accelerating aging procedures, the ARRHENIUS model is a well-established approach to account for this effect. However, aging caused by exposure to CL is a specific issue with a limited range of applications and, as such, has not been extensively modeled. Consequently, no equivalent ARRHENIUS model

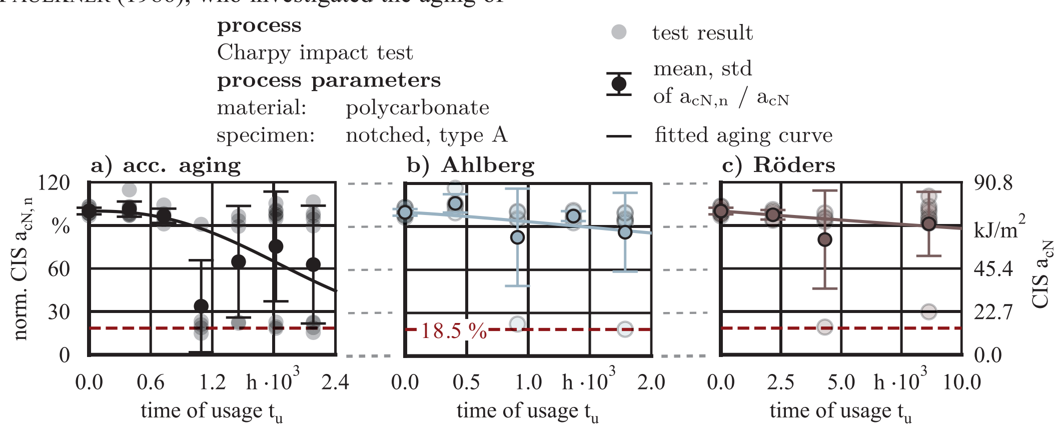

Fig 4. Charpy impact test results; a) Accelerated aging; b) Aging under industrial conditions by Ahlberg; c) Aging under industrial conditions by Röders.

exists to compensate for the effects of elevated CL concentrations σ. Instead, an approach similar to that proposed by HAMID AND AMIN (1995), which calculates a shift factor based on the time required to reach a characteristic value, is employed. To derive a concentration shift factor f_c, the characteristic aging time (CAT) t_∞, defined as the time at which the aging curve reaches the fatigue lower limit $a_{cN,n\infty}$, is determined for all aging curves. Additionally, the temperature shift factor f_t is applied to the CAT of the accelerated aging procedure $t_{\infty,acc}$. The concentration shift factor f_c is subsequently calculated as shown in Eq. (6), where $t_{\infty,R}$ and $t_{\infty,A}$ represent the CAT for the aging curves of Röders and Ahlberg, respectively.

$$f_c = \left[t_{\infty,acc} / f_t\right] / \left[\left(t_{\infty,A} + t_{\infty,R}\right) / 2\right] \qquad (6)$$

Using the CAT t_∞ shown in Table 3, the concentration shift factor is calculated as $f_c = 1.61 \cdot 10^{-1}$.

Table 3. CAT t_∞ used for calculation of the concentration shift factor f_c.

$t_{\infty,acc}$ in h	$t_{\infty,A}$ in h	$t_{\infty,R}$ in h
$4.10 \cdot 10^3$	$2.93 \cdot 10^4$	$2.94 \cdot 10^5$

The original aging curves for all aging procedures, along with the temperature- and concentration-corrected aging curve, are presented on a logarithmic time scale in Fig 5.

<u>Safeguard impact tests</u>

The above paragraph demonstrated the derivation of an aging curve and its transformation to industrial operating condition in machine tools using a temperature shift factor f_t and concentration shift factor f_c based on Charpy impact tests.

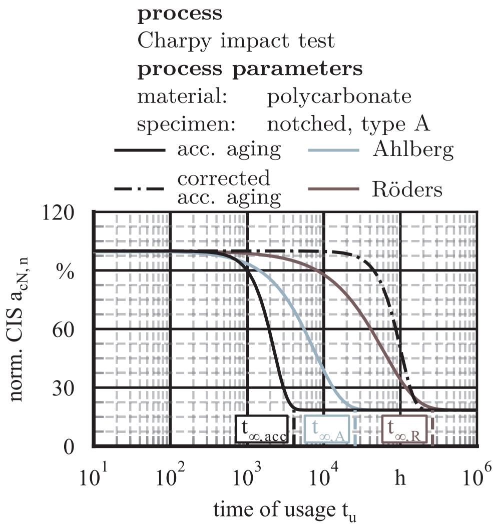

Fig 5. Comparison of original and temperature- and concentration-corrected aging curve.

This framework is now applied to the results of safeguards impact tests, as it is reasonable to assume that the Charpy specimens experienced the same accelerated aging effects as the PC sheets. A comparison between the results of Charpy impact tests and safeguard impact tests is presented in Fig 6. When comparing the decrease of normalized CIS $a_{cN,n}$ shown in Fig 6a) to the decrease of normalized BLV $v_{bl,n}$ depicted in Fig 6b), three key observations can be made:

- The decrease in normalized BLV $v_{bl,n}$ is significantly less pronounced than the decrease in normalized CIS $a_{cN,n}$.
- Similar to the Charpy impact tests the fatigue lower limit $v_{bl,\infty}$ has not been reached in the experiments.

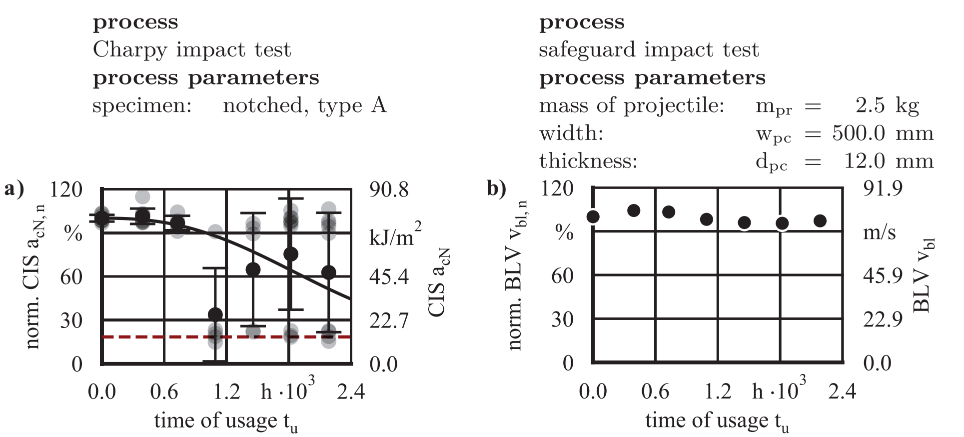

Fig 6. Degradation of PC under accelerated conditions: a) Normalized CIS $a_{cN,n}$; b) Normalized BLV $v_{bl,n}$.

- In contrast to the Charpy impact tests there are not particular low values around which the safeguard impact tests tend to cluster.

The first observation can be attributed to the fact that CL-related aging of PC primarily occurs at or near the material's surface. Since Charpy specimens have a higher surface-to-volume ratio, aging affects a greater percentage of their volume. In contrast, the thicker PC sheets are less impacted by CL exposure, resulting in a less pronounced decrease in BLV v_{bl} due to aging. Again, the detailed mechanisms of the aging process will be presented in future work, as they are beyond the scope of the present study. While this observation can be addressed by adjusting the parameters α and β of the aging curve, the second and third observations pose a more significant challenge, as the aging curve cannot be defined without a fatigue lower limit $v_{bl,n\infty}$. However, it is plausible to assume that PC sheets would experience aging effects similar to those observed in Charpy specimens, given a sufficiently long time of usage t_u. In the absence of a more accurate value the fatigue lower limit $v_{bl,\infty}$ is assumed to be the same for both Charpy and safeguard impact tests. This assumption ultimately allows for the definition of an aging curve for PC sheets used as safeguards in machine tools with its parameters shown in Table 4.

Table 4. Coefficients of aging curve for safeguards.

$v_{bl,n0}$	$v_{bl,n\infty}$	α	β
1.00	$1.85 \cdot 10^{-2}$	$7.59 \cdot 10^{-2}$	2.06

Since the effect of elevated temperature ϑ and CL concentration σ is the same regardless of the testing procedure, both the temperature shift factor f_t and the concentration shift factor f_c are applied to the aging curve of safeguards. The original aging curve and the temperature- and CL concentration-corrected aging curve is shown alongside the aging curve from ISO 23125 in Fig 7. While both aging curves exhibit a comparable shape, they differ in terms of their respective fatigue lower limits $v_{bl,n\infty}$ and decay rates. The fatigue lower limit for the ISO 23125 aging curve is $v_{bl,n\infty} = 2$ %, whereas the updated aging curve proposed in this study has a fatigue lower limit of $v_{bl,n\infty} = 18.5$ %. More importantly, the characteristic degradation time t_d when the PC vision

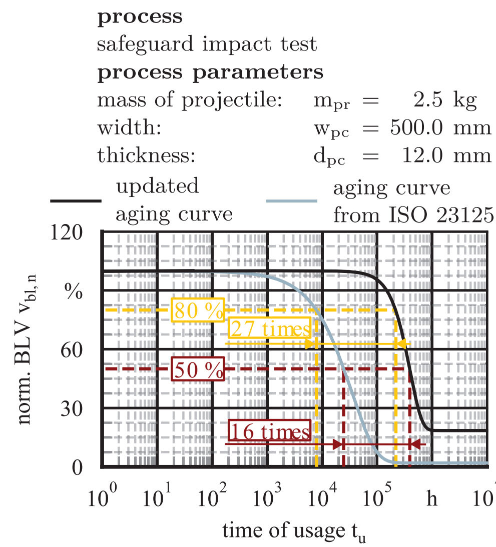

Fig 7. Comparison of updated and current aging curve from ISO 23125.

panels lose 80 % / 50 % of their initial normalized BLV $v_{bl,n}$ is reached 27 or 16 times later in the updated aging curve. In other words, for VSI 034, the updated aging curve allows for a significantly longer time of usage, as the CL-related decrease in BLV v_{bl} is overestimated by the current aging curve from ISO 23125.

3. Conclusion and Outlook

The primary objective of this paper was to derive a new aging curve for PC vision panels exposed to CL in machine tools. To achieve this, two aging experiments were analyzed using Charpy impact tests and safeguard impact tests in accordance with ISO 23125. This study demonstrated how the results of accelerated aging procedures can be mapped onto industrial operating conditions using temperature and concentration shift factors. It was found that the currently available aging curve significantly overestimates the actual aging of PC vision panels for the investigated CL. Moreover, the framework presented in this paper can be extended to other CL formulations. Ongoing accelerated aging experiments are currently being conducted and will be analyzed in the future to validate the aging curve presented in this paper.

Acknowledgement

The project is funded by the Federal Ministry for Economic Affairs and Climate Action based on a resolution of the German Bundestag. The authors extend their gratitude also to Ahlberg Engineering GmbH and Röders GmbH for their participation.

References

Albert, Wilhelm August Julius. 1837. “Ueber Treibseile Am Harz.” Archiv Für Mineralogie, Geognosie, Bergbau Und Huttenkunde 10:215-34.

Ben-Dor, Gabi, Anatoly Dubinsky, and Tov Elperin. 2006. Applied High-Speed Plate Penetration Dynamics. Solid Mechanics and Its Applications, v. 132. Dordrecht: Springer.

Bold, Jörg. 2004. “Trennende Schutzeinrichtungen Für Werkzeugmaschinen Zur Hochgeschwindigkeits-bearbeitung.” Berlin: Technische Universität Berlin.

Burhan, Ibrahim, and Ho Sung Kim. 2018. “S-N Curve Models for Composite Materials Characterisation: An Evaluative Review.” Journal of Composites Science 2 (3): 38.

Collins, David, Jason Freels, Aparna Huzurbazar, Richard Warr, and Brian Weaver. 2013. “Accelerated Test Methods for Reliability Prediction.” Journal of Quality Technology 45 (July):244–59.

Ehrenstein, Gottfried Wilhelm, and Sonja Pongratz. 2007. “Beständigkeit von Kunststoffen.” In *Beständigkeit von Kunststoffen*, I–XIX. Carl Hanser Verlag GmbH & Co. KG.

Faulkner, Douglas L. 1986. “The Role of Surfactant Structure and Monoethanolamine in the Environmental Stress Cracking of Polycarbonate.” *Journal of Applied Polymer Science* 32 (5): 4909–17.

Golovoy, A., and M. Zinbo. 1989. “Water Sorption and Hydrolytic Stability of Polycarbonates.” Polymer Engineering & Science 29 (24): 1733–37.

Hamid, S. H., and M. B. Amin. 1995. “Lifetime Prediction of Polymers.” Journal of Applied Polymer Science 55 (10): 1385–94.

Ising, Michael. 1997. “Dimensionierung Und Gestaltung Trennender Schutzeinrichtungen.” Berlin: Institut für Werkzeugmaschinen und Fabrikbetrieb.

Kahlen, S., G. M. Wallner, and R. W. Lang. 2010. “Aging Behavior and Lifetime Modeling for Polycarbonate.” Solar Energy 84 (5): 755–62.

Kim, Ho-Sung, and Jianping Zhang. 2001. “Fatigue Damage and Life Prediction of Glass/Vinyl Ester Composites.” Journal of Reinforced Plastics and Composites 20 (July):834–48.

Lambert, J. P., and G. H. Jonas. 1976. “Towards Standardization in Terminal Ballistics Testing: Velocity Representation:” Fort Belvoir, VA: Defense Technical Information Center.

ISO 179-1:2023 - Determination of Charpy impact properties - Part 1: Non-instrumented impact test. 2023. Geneva: Internation Organization for Standardisation.

ISO 14120:2015 - Safety of Machiniery - General Requirements for the Design And Construction Fixed And Movable Guards. 2015. Geneva: Internation Organization for Standardisation.

ISO 23125:2015 - Machine Tools - Safety - Turning Machines. 2015. Geneva: Internation Organization for Standardisation.

Pickett, James E., and Dennis J. Coyle. 2013. “Hydrolysis Kinetics of Condensation Polymers under Humidity Aging Conditions.” Polymer Degradation and Stability 98 (7): 1311–20.

Recht, R. F., and T. W. Ipson. 1963. “Ballistic Perforation Dynamics.” Journal of Applied Mechanics 30 (3): 384–90.

Schütz, Walter. 1996. “A History of Fatigue.” Engineering Fracture Mechanics 54 (2): 263–300.

Sendeckyj, G. P. 1981. “Fitting Models to Composite Materials Fatigue Data.” Test Methods and Design Allowables for Fibrous Composites, January, 245–60.

Starkova, Olesja, Abedin I. Gagani, Christian W. Karl, Iuri B. C. M. Rocha, Juris Burlakovs, and Andrey E. Krauklis. 2022. “Modelling of Environmental Ageing of Polymers and Polymer Composites - Durability Prediction Methods.” Polymers 14 (5): 907.

Uhlmann, E., M. Polte, R. Hörl, N. Bergström, S. Thom, and P. Wittwer. 2021. “Experimental Investigation of The Kink Effect by Impact Tests on Polycarbonate Sheets.” In Proceedings of the 31st European Safety and Reliability Conference (ESREL 2021), 1253–61. Research Publishing Services.

Uhlmann, Eckart, Nils Bergström, Caroline Demidova, and Florian Meurer. 2024. “Logistic Regression In Practice: Determining Impact Resistance Of Polycarbonate Vision Panels With Limited Data Set.” In Advances in Reliability, Safety and Security, Part 3, 183–90. Cracow.

Uhlmann, Eckart, Mitchel Polte, Nils Bergström, and Vu Ninh Le. 2023. “Modeling the Age-Related Decrease in Ballistic Limit Velocity of Polycarbonate Vision Panels Using a Johnson-Cook Material Model Coupled with Variable Failure Criteria.” Journal of Machine Engineering, no. 23 (June).

Weibull, Waloddi. 1952. “The Statistical Aspect of Fatigue Failures and Its Consequences.” Fatigue and Fracture of Metals, 182–96.

Wöhler, August. 1858. “Bericht Über Die Versuche, Welche Auf Der Königl. Niederschlesich-Märkischen Eisenbahn Mit Apparaten Zum Messen Der Biegung Und Verdrehung Von Eisenbahnwagenachsen Während Der Fahrt Angestellt Wurden.” Zeitschrift Für Bauwesen 8:641–52.

Wöhler, August. 1860. “Versuche Zur Ermittlung Der Auf Die Eisenbahnachsen Einwirkenden Kräfte Und Die Widerstandsfähigkeit Der Wagen-Achsen.” Zeitschrift Für Bauwesen 10:583–161.